Domain structures of $PbTiO_3$ and $Pb(Zr,Ti)O_3$ thin films controlled by tensile strain induced by a $Sr(Zr,Ti)O_3$ buffer layer

Tomohide Morikawa[1], Masanori Kodera[2, † a)], Takao Shimizu[3], Keisuke Ishihama[1], Yoshitaka Ehara[4], Osami Sakata[5], and Hiroshi Funakubo[1,2 a)]

[1] *School of Materials and Chemical Technology, Tokyo Institute of Technology, Yokohama 226-8502, Japan*

[2] *Material Research Center for Element Strategy, Tokyo Institute of Technology, Yokohama, 226-8502, Japan*

[3] *Research Center for Functional Materials, National Institute for Materials Science, Tsukuba, 305-0044, Japan.*

[4]*Department of Communications Engineering, National Defense Academy, Hashirimizu, Yokosuka, 239-8686, Japan.*

[5] *Center for Synchrotron Radiation Research, Japan Synchrotron Radiation Research*

Institute (JASRI) SPring-8, 1-1-1 Kouto, Sayo-cho, Sayo-gun 679-5198, Hyogo, Japan

† *Present address: Global Zero Emission Research Center, National Institute of Advanced Industrial Science and Technology, Tsukuba West, 16-1, Onogawa, Tsukuba, Ibaraki, 305-8569 Japan*

a) Electronic mail: funakubo.h.aa@m.titech.ac.jp

Keywords: epitaxial thin films, ferroelectrics, domain engineering, tensile strain

Abstract:

Thin films of $Sr(Zr,Ti)O_3$ were investigated as buffer layers to induce tensile strain in ferroelectric thin films such as $PbTiO_3$ and $Pb(Zr,Ti)O_3$ to control the domain structure. By tuning the composition of $Sr(Zr,Ti)O_3$, (100)-oriented $PbTiO_3$ and $Pb(Zr,Ti)O_3$ films were obtained, revealing that tensile strain was introduced into the thin films by the lattice of the buffer layer. We propose a methodology for the successive control of tensile stress, which is useful for understanding and controlling the domain structures of ferroelectric films that result in the ferroelectric and piezoelectric properties of ferroelectric thin films.

(93 words)

Ferroelectric films have been used as a component in many devices, such as non-volatile memories, piezoelectric actuators, sensors, and energy harvesters.[1–3] To connect all things to the Internet, trillions of electric devices with superior properties are demanded.[4] Recently, single-crystalline epitaxial films have drawn attention owing to their potentially superior electrical and electromechanical properties compared with those of a polycrystalline bulk form.[5,6] In ferroelectric films, the domain structure plays a critical role in determining ferroelectric, piezoelectric, and dielectric properties, which can be controlled by the strain induced from the bottom layer, which is usually a substrate.[5,7–9]

The effects of induced strain on the domain structure were investigated in detail theoretically for tetragonal ferroelectrics. A large compressive strain affords (001)-orientation with out-of-plane polarization while a tensile strain causes (100)/(010)-orientation with in-plane polarization; these are denoted as *c*-domain and *a*-domain, respectively.[10] In terms of experimental reports, although the effects of strain induced from single-crystalline substrates on the domain structures were investigated for several decades, a comprehensive understanding and control of the domain structure has not yet been accomplished. For instance, $Pb(Zr_xTi_{1-x})O_3$ (PZT, x>0.2) with a pure *a*-domain has never been realized. One of the reasons for this is that the choice of single-crystal substrates to introduce tensile strain to films is limited, especially those with large lattice constants. Moreover, their lattice constants are discrete, making it challenging to precisely control the degree of strain. To introduce tensile strain in PZT (x>0.3), which is the most important ferroelectric material, lattice constants larger than 0.4 nm are desired.

Hence, only a few papers have reported $PbTiO_3$ (PT, PZT x=0) with a pure *a*-domain prepared on $KTaO_3$ (KTO)[11–13] and $SmScO_3$ single-crystal substrates.[14] The pure *a*-domain is only observed in an extremely thin film thickness,[15] and the *a*-domain is converted to a *c*/*a*-polydomain structure with increasing film thickness.[12,14,16–18] Recently, our group succeeded in preparing *a*-domain

PT films (thickness：2-90 nm) grown on KTO substrates.[19] However, even when the KTO single crystals were used as substrates, PZT with a near-morphotropic phase boundary (MPB)(PZT x~0.52, larger lattice parameter than KTO substrates) region should exhibit the c-domain due to the application of compressive stress to the films.[10,13] Although some perovskite-type oxides have sufficiently large lattice constants to introduce tensile strain into PZT, their single-crystalline substrates are not easily available. Therefore, we considered using these oxides as buffer layers to control domain structures. Compared with the domain engineering of films directly grown on single-crystalline substrates, domain engineering using a buffer layer is very limited, probably owing to a high technical barrier to obtaining high-quality films.

A cubic structure was desired as a buffer layer to ensure isotropic conditions for the investigation of domain structures. The tetragonality (calculated as the ratio of the longer lattice distance to the shorter one, c/a) should be close to 1. Sc-based perovskite-type oxides, such as $DyScO_3$ and $SmScO_3$ have relatively good small tetragonality (1.001–1.003).[20,21] For example, the tetragonalities of $NdScO_3$ and $GdScO_3$ are 1.003 and 1.001, respectively. In addition, the buffer layer should be chemically and thermodynamically stable and should not react with either the substrate or films.

Herein, we focus on a buffer layer, $Sr(Zr_yTi_{1-y})O_3$ (denoted as SZT, y=0, 0.43, 0.65, and 0.9), to induce tensile strain in a wide range of PZT films ($0<x<0.5$). First, we confirmed the properties of SZT. $PbTiO_3$ (PT) and PZT films were then prepared on the SZT-buffered substrates. Although the crystal structure of SZT changes from cubic ($Pm3m$) to orthogonal ($Pbnm$) via tetragonal ($I4/mcm$) with increasing zirconium ratio (y), SZT has a very small tetragonality of almost unity (Table S1).[22] This tetragonality is comparable to or even better than that of $DyScO_3$ and $NdScO_3$. Lattice constants of SZT can be controlled from 0.3905 nm (STO) to 0.41 nm (cubic-equivalent SZ), therefore, it is expected that the SZT can induce both compressive and tensile strain to a wide composition range of PZT films ($0<x<0.5$). Moreover, lattice constants can be continuously and precisely controlled by tuning the composition, which should be a great advantage to use buffer layer. Although SZT has been

reported as a potential buffer layer, no study has experimentally proved that SZT acts as a buffer layer to induce tensile strain in ferroelectric films.

SZT (y=0, 0.43, 0.65, and 0.9) films were prepared by a pulsed laser deposition (PLD) technique. Single-crystalline $SrTiO_3$ and $(LaAlO_3)_{0.3}$-$(SrAl_{0.5}Ta_{0.5}O_3)_{0.7}$ (LSAT) were heated to 973 K under 0.01 Torr of O_2 atmosphere. An excimer laser (λ=248 nm) was irradiated with a frequency of 4 to 10 Hz. The laser energy was set to 250 mJ.

The PT films were deposited by pulsed metal–organic chemical vapor deposition (MOCVD). The obtained films were characterized by ω-2θ X-ray diffraction (XRD, PANalytical) scan and reciprocal space mapping (RSM) obtained from a 2θ-*psi* scan using a D8-Discover (Bruker) equipped with a 2D detector. *H-K* mapping of PT was obtained using a synchrotron X-ray source (SPring-8, 12.4 keV, scintillation counter). Piezoforce microscopy (PFM; Cypher, vector mode) was used to observe the domain structure.

First, the deposition conditions for SZT on single-crystalline STO and LSAT substrates were optimized. As a buffer layer, the SZT should exhibit a stable lattice constant for film deposition. Therefore, the film thickness must be sufficiently large for the lattice parameters to reach saturation in the bulk. By contrast, in terms of surface roughness, a thinner surface is likely to be better. Thus, a trade-off exists between these two factors. For example, the optimal thickness of the SZT(y=0.65) was 150 nm for STO (See Fig. S1 in the Supporting Information). Notably, the optimized thicknesses of SZT on the LSAT were smaller than those of SZT/STO. SZT/LSAT has a larger lattice mismatch between the buffer layer and substrate than the SZT/STO system, which reduces the thickness of the lattice parameter.

After optimizing the deposition conditions of SZT, PT thin films were deposited on the buffered substrates to investigate whether the a_1/a_2 domain was formed by tensile strain from the buffer layer. It should be noted that SZT (y=0.43, a=0.399 nm) had an almost identical lattice constant to that of KTO (a=0.399 nm). Figure 1 shows the XRD patterns of the PT films deposited on the optimized SZT/STO and SZT/LSAT films with several SZT compositions. The PT film thickness was

approximately 30 nm.

In all cases, only peaks corresponding to SZT, PT, and the substrates were observed. The peak position of the SZT shifted to a lower angle as y increased, indicating that the out-of-plane lattice constants of the SZT buffer layer increased. Moreover, the observed lattice constants are in good agreement with the reported values for the SZT powder. Therefore, the SZT buffer layers were likely relaxed.

Regardless of the SZT composition and substrate used, only one peak attributable to 100 diffraction from PT was observed, suggesting that (100)/(010)-oriented films were obtained without other orientations. The peak positions of SZT were similar before and after PT deposition, suggesting that SZT does not react strongly with PT or the substrates during deposition.

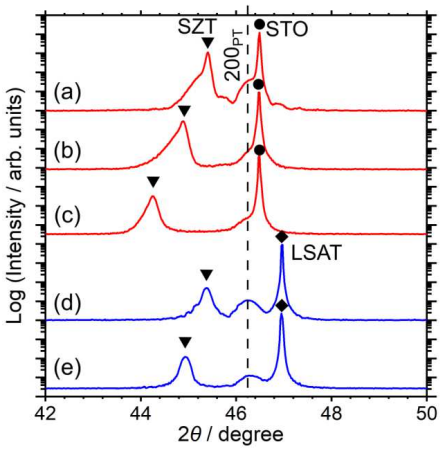

Fig. 1. XRD patterns for (a) PT/SZT(y=0.43)/STO, (b) PT/SZT(y=0.65)/STO, (c) PT/SZT(y=0.90)/STO, (d) PT/SZT(y=0.43)/LSAT, and (e) PT/SZT(y=0.65)/LSAT

Next, asymmetric and symmetric RSM were obtained, as shown in Fig. 2, because symmetric XRD measurements do not reflect the properties of the in-plane direction. From the RSM near 200_{STO}, only two spots were observed: 200_{SZT} and 200_{STO}. As shown in Fig. 1, the spots from

200_{PT} almost overlapped with those from 200_{STO}, resulting in no apparent spots. By contrast, Fig. 2(c) shows three clear spots because LSAT exhibits a smaller lattice constant than that of STO and PT, and the spots do not overlap. In both cases, there was no spot from 002_{PT}, which corresponds to the results shown in Fig. 1.

The asymmetric RSMs near the 220_{STO} region are shown in Figs. 2 (d–f). Both STO and SZT are located on the cubic line (i.e., $q_x=q_z$), indicating the complete relaxation of the lattice constants of SZT. Furthermore, clear spots attributable to 202_{PT} were observed without any spots from 022_{PT}, which strongly supported the lack of a *c*-domain. Thus, the PT films prepared on the SZT buffer layers exhibit an *a*-domain without a *c*-domain.

Although many papers have reported domain structures on a buffer layer, such as PZT/SRO/STO, the buffer layer acts as a conductive or seed layer to help epitaxial growth.[23,24] Therefore, this is the example of obtaining a PT film with only the *a*-domain stabilized by the tensile strain induced by the buffer layer.

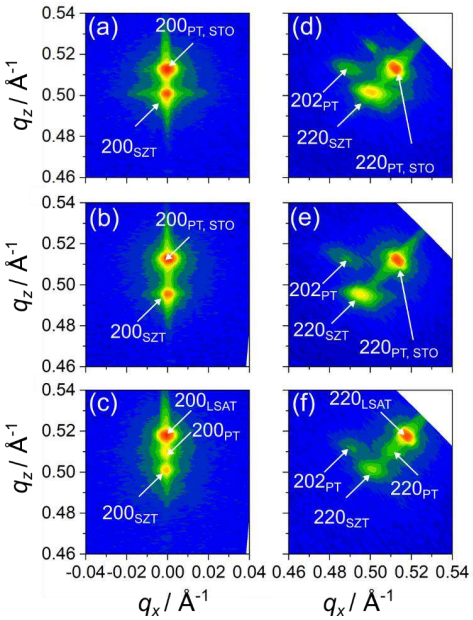

Fig. 2. XRD-RSM for (a, d) PT/SZT(y=0.43)/STO, (b, e) PT/SZT(y=0.65)/STO and (c, e) PT/SZT(y=0.43)/LSAT. (a, b, c) mapping around 200_{STO} and (d, e, f) mapping around 202_{STO}

To further investigate the domain structure, *H-K* mapping was performed using synchrotron radiation at SPring-8 (Fig. 3). To prevent damage caused by intense X-ray radiation to the detector, the area near the STO substrate was excluded from the measurement range. *H-K* mapping can show the cross section of the reciprocal space at a certain *L* value, as shown in Fig. S3. To avoid strong reflection from the STO substrates, *H-K* mapping around $L=2_{STO}$ was recorded, except near the STO spots. Figure 3a shows 4 clear spots from 200_{PT} and 020_{PT} as well as a strong spot at the center of the four spots. It is confirmed that the strong spot was not attributable to SZT by scanning along the *L*-axis at (*H*, *K*)=(1.96 r. l. u, 0 r. l. u.). Therefore, a strong spot is likely to stem from the periodic structure of the a_1/a_2-domain.[11,25] For PT/SZT(y=0.65)/STO and PT/SZT(y=0.43)/LSAT, similar figures were obtained. The peak intensity around H_{STO}=2.00 was higher than that at H_{STO}=1.90 in Figs.

3(b, c). The tail of a prominent peak from the substrate may be overlapping. Although measurement configurations were carefully set up to ensure that the sample surface was parallel to the H-K plane; however, there may have been a slight deviation, resulting in the asymmetric figure. Moreover, four spots from the a_1/a_2-domain are observed, they exhibit different streak directions. Although the reason for these results has not been fully elucidated, one possible explanation is that the a_1/a_2-domain is slightly tilted because of the tetragonality of SZT.

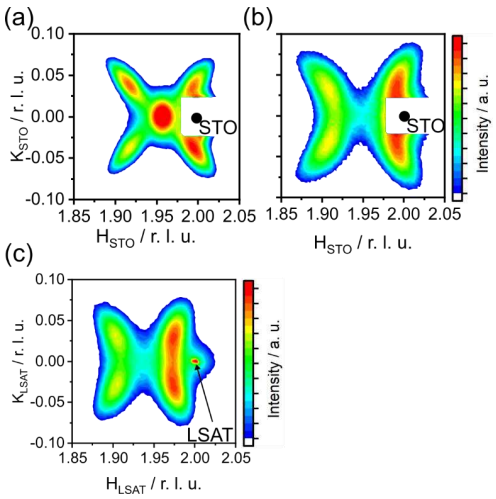

Fig. 3. XRD *H-K* mappings for (a) PT/SZT(y=0.43)/STO, (b) PT/SZT(y=0.65)/STO and (c) PT/SZT(y=0.43)/LSAT using synchrotron irradiation

In addition to XRD-based analysis, PFM was performed to clarify the domain configuration shown in Fig. 4. In both Figs. 4a and 4b, an obvious contrast from the a_1/a_2-domain was observed in the amplitude images, which is in good agreement with that reported for PT/KTO[11] and PT/$GdScO_3$.[26] Moreover, the amplitude and phase images are not observed in *a/c*-superdomain patetrns[14], which is also supporting the formation of the a_1/a_2-domain without a *c*-domain. Although the a_1/a_2-super domain boundaries in the lateral images contained nonuniformity, this was likely caused by the surface

roughness of the films. Thus, the introduction of tensile strain into the film using the SZT buffer layer was directly confirmed.

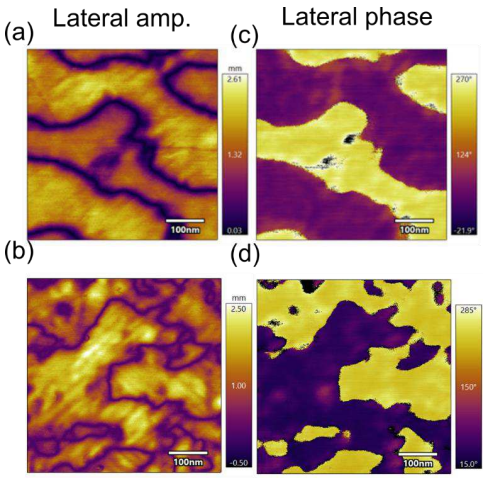

Fig. 4. PFM images of (a, b) lateral amplitude and (c, d) lateral phase for (a, c) PT/SZT(y=0.43)/STO and (b, d) PT/SZT(y=0.43)/LSAT

Finally, PZT(x=0.3)/SZT/STO was prepared to confirm the formation of the a_1/a_2-domain under tensile strain. Figure 5 shows the XRD patterns of PZT(x=0.3)/SZT/STO with SZT compositions ranging from y=0 (STO) to y=0.9. The composition of the buffer layer critically affected the domain structure of the PZT film. For example, PZT(x=0.3)/STO only exhibited a c-domain, as in a previous report[20], whereas PZT(x=0.3)/SZT(y=0.43)/STO contained both a- and c-domains. Furthermore, it should be emphasized that $Pb(Zr_{0.3}Ti_{0.7})O_3$ which comprised only the a-domain was experimentally realized unprecedentedly using an SZT(y=0.65) buffer layer, thereby, accomplishing the successive control of the domain structure from a-domain to c-domain. It should be noted that clear PFM images were not obtained so far, which is likely due to the relatively large surface roughness. Therefore, the optimization of experimental conditions for both SZT and PZT deposition should be investigated in the future work.

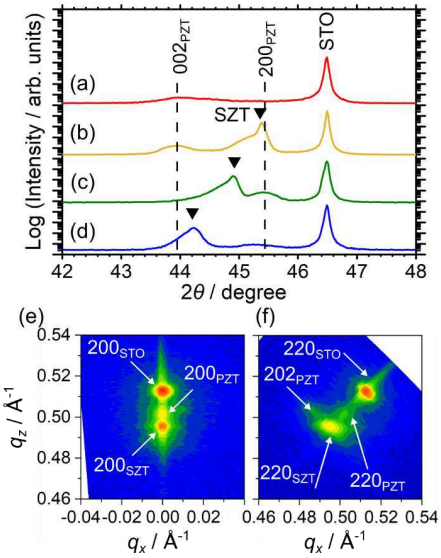

Fig. 5 (a-d) XRD patterns and (e, f) RSM images for (a) PZT(x=0.3)/STO, (b) PZT(x=0.3)/SZT(y=0.43)/STO, (c, e, f) PZT(x=0.3)/SZT(y=0.65)/STO, and (d) PZT(x=0.3)/SZT(y=0.9)/STO

Recently, films comprising solely the *a*-domain have drawn attention because of their potential advantages in SAW devices or actuators that use the in-plane piezoelectric mode.[27] Therefore, this study provides fruitful results for understanding the fundamentals in domain engineering and a practically important methodology to obtain PZT films with a_1/a_2-domain for superior dielectric/ferroelectric properties. To further develop this methodology, the properties of the buffer layers, such as the film roughness, crystallinity, and orientation, need to be improved.

Another potential direction for further advancing this research is the development of a conductive buffer layer to measure dielectric, piezoelectric, and ferroelectric properties in the film thickness direction.

In conclusion, we demonstrated the concept of controlling the domain structure of ferroelectric films, in which SZT functioned as an effective buffer layer to introduce compressive and tensile strains in a wide range of PZT films. Our results should enrich the scope of studies on the domain engineering of ferroelectric materials.

See the supplementary material for details about the tetragonality of SZT with various compositions and calculated lattice parameters and surface roughness (Ra) for SZT(y=0.65)/STO with various SZT thicknesses, and also refer to the schematic of H-K mapping in reciprocal space.

Acknowledgment

This work was partially supported by the Element Strategy Initiative to Form a Core Research Center of the Ministry of Education, Culture, Sports, Science, and Technology of Japan (MEXT; Grant Number JPMXP0112101001). This work was also supported by JSPS KAKENHI Grant Numbers 19K15288 (TS) and 23KJ0903 (KI), and MEXT KAKENHI Grant Number 20H05185 (TS). Synchrotron radiation experiments were performed at the BL15XU beamline of SPring-8 with the approval of the Japan Synchrotron Radiation Research Institute (Proposal No. 2020A4950, 2019A4903, and 2020A4551). One of the authors thanks the support from Murata Science and Education Foundation.

Data Availability Statement

The data that support the findings of this study are available from the corresponding author upon reasonable request.

Author contributions

Tomohide Morikawa: analysis (lead); investigation (lead); review and editing (equal). Masanori Kodera: project administration (supporting); writing – original draft (lead); analysis (supporting)

investigation (supporting); writing – review and editing (equal). Takao Shimizu: conceptualization (lead), funding acquisition (supporting); review and editing (equal). Keisuke Ishihama: investigation (supporting); funding acquisition (supporting); writing – original draft (supporting); review and editing (equal). Yoshitaka Ehara: investigation (supporting); review and editing (equal). Osami Sakata: investigation (supporting); review and editing (equal). Hiroshi Funakubo: funding acquisition (lead); supervision (lead); conceptualization (supporting); project administration (lead) review and editing (equal).

Conflict of Interests Statement

There is no conflict to declare.

References

[1] T. Mikolajick, U. Schroeder, and S. Slesazeck, "The Past, the Present, and the Future of Ferroelectric Memories," IEEE Trans Electron Devices **67**(4), 1434–1443 (2020).

[2] S. Trolier-Mckinstry, F. Griggio, C. Yaeger, P. Jousse, D. Zhao, S.S.N. Bharadwaja, T.N. Jackson, S. Jesse, S. V. Kalinin, and K. Wasa, "Designing piezoelectric films for micro electromechanical systems," IEEE Trans Ultrason Ferro. Freq Control **58**(9), 1782–1792 (2011).

[3] G.T. Hwang, M. Byun, C.K. Jeong, and K.J. Lee, "Flexible piezoelectric Thin-Film energy harvesters and nanosensors for biomedical applications," Adv Healthc Mater **4**(5), 646–658 (2015).

[4] T. Mikolajick, S. Slesazeck, H. Mulaosmanovic, M.H. Park, S. Fichtner, P.D. Lomenzo, M. Hoffmann, and U. Schroeder, "Next generation ferroelectric materials for semiconductor process integration and their applications," J. Appl. Phys. **129**(10), (2021).

[5] Y.S. Oh, L. Wang, H. Lee, W.S. Choi, and T.H. Kim, "Polar Perturbations in Functional Oxide Heterostructures," Adv. Funct. Mater. **2302261**, 1–32 (2023).

[6] K.J. Choi, M. Biegalski, Y.L. Li, A. Sharan, J. Schubert, R. Uecker, P. Reiche, Y.B. Chen, X.Q. Pan, V. Gopalan, L.Q. Che, D.C. Schlom, and C.B. Eom, "Enhancement of ferroelectricity in strained $BaTiO_3$ thin films," Science **306**(5698), 1005–1009 (2004).

[7] P.E. Janolin, "Strain on ferroelectric thin films : EEEExample of $Pb(Zr_{1-x}Ti_x)O_3$," J Mater Sci **44**(19), 5025–5048 (2009).

[8] S.-G. Cao, H.-H. Wu, H. Ren, L.-Q. Chen, J. Wang, J. Li, and T.-Y. Zhang, "A novel mechanism to reduce coercive field of ferroelectric materials via {111} twin engineering," Acta Mater **97**, 404–412 (2015).

[9] V. Shelke, D. Mazumdar, G. Srinivasan, A. Kumar, S. Jesse, S. Kalinin, A. Baddorf, and A. Gupta, "Reduced Coercive Field in $BiFeO_3$ Thin Films Through Domain Engineering," Adv. Mater. **23**(5), 669–672 (2011).

[10] V.G. Kukhar, N.A. Pertsev, H. Kohlstedt, and R. Waser, "Polarization states of polydomain epitaxial $Pb(Zr_{1-x}Ti_x)O_3$ thin films and their dielectric properties," Phys Rev B **73**(21), 214103 (2006).

[11] D. Ichinose, T. Shimizu, O. Sakata, T. Yamada, and H. Funakubo, "Domain structure transition from two to three dimensions in tensile strained (100)/(001)-oriented epitaxial tetragonal PZT film," Appl. Phys. Lett. **113**(13), 132905 (2018).

[12] T. Nakashima, D. Ichinose, Y. Ehara, T. Shimizu, T. Kobayashi, T. Yamada, and H. Funakubo, "Effect of in-plane tensile strain in (100)/(001)-oriented epitaxial $PbTiO_3$ films

on their phase transition temperature and tetragonal distortion," Appl. Phys. Lett. **110**(12), 122902 (2017).

[13] D. Ichinose, T. Nakashima, Y. Ehara, T. Oikawa, T. Shimizu, O. Sakata, T. Yamada, and H. Funakubo, "Orientation control of epitaxial tetragonal $Pb(Zr_xTi_{1-x})O_3$ thin films grown on (100)$KTaO_3$ substrates by tuning the Zr/(Zr+Ti) ratio," Appl. Phys. Lett. **107**(2), 022902 (2015).

[14] E. Langenberg, H. Paik, E.H. Smith, H.P. Nair, I. Hanke, S. Ganschow, G. Catalan, N. Domingo, and D.G. Schlom, "Strain-Engineered Ferroelastic Structures in $PbTiO_3$ Films and Their Control by Electric Fields," ACS Appl Mater. Interfaces. **12**(18), 20691–20703 (2020).

[15] Q.Y. Qiu, V. Nagarajan, and S.P. Alpay, "Film thickness versus misfit strain phase diagrams for epitaxial $PbTiO_3$ ultrathin ferroelectric films," Phys. Rev. B **78**(6), 064117 (2008).

[16] A.R. Damodaran, S. Pandya, J.C. Agar, Y. Cao, R.K. Vasudevan, R. Xu, S. Saremi, Q. Li, J. Kim, M.R. McCarter, L.R. Dedon, T. Angsten, N. Balke, S. Jesse, M. Asta, S. V. Kalinin, and L.W. Martin, "Three-State Ferroelastic Switching and Large Electromechanical Responses in $PbTiO_3$ Thin Films," Adv. Mater. **29**(37), 1702069 (2017).

[17] O. Nesterov, S. Matzen, C. Magen, A.H.G. Vlooswijk, G. Catalan, and B. Noheda, "Thickness scaling of ferroelastic domains in $PbTiO_3$ films on $DyScO_3$," Appl Phys Lett **103**(14), 142901 (2013).

[18] A.H.G. Vlooswijk, B. Noheda, G. Catalan, A. Janssens, B. Barcones, G. Rijnders, D.H.A. Blank, S. Venkatesan, B. Kooi, and J.T.M. de Hosson, "Smallest 90° domains in epitaxial ferroelectric films," Appl. Phys. Lett. **91**(11), 112901 (2007).

[19] Y. Ehara, T. Nakashima, D. Ichinose, T. Shimizu, T. Shiraishi, O. Sakata, T. Yamada, S. Yasui, K. Nishida, and H. Funakubo, "Film thickness dependence of in-plane ferroelastic domain structure in constrained tetragonal $PbTiO_3$ films induced by isotropic tensile strain," Appl. Phys. Lett. **121**(26), (2022).

[20] M.D. Biegalski, J.H. Haeni, S. Trolier-McKinstry, D.G. Schlom, C.D. Brandle, and A.J. Ven Graitis, "Thermal expansion of the new perovskite substrates $DyScO_3$ and $GdScO_3$," J. Mater. Res. **20**(4), 952–958 (2005).

[21] R. Uecker, H. Wilke, D.G. Schlom, B. Velickov, P. Reiche, A. Polity, M. Bernhagen, and M. Rossberg, "Spiral formation during Czochralski growth of rare-earth scandates," J. Cryst Growth **295**(1), 84–91 (2006).

[22] T.K.Y. Wong, B.J. Kennedy, C.J. Howard, B.A. Hunter, and T. Vogt, "Crystal structures and phase transitions in the $SrTiO_3$-$SrZrO_3$ solid solution," J. Solid State Chem. **156**(2), 255–263 (2001).

[23] S. Yokoyama, Y. Honda, H. Morioka, S. Okamoto, H. Funakubo, T. Iijima, H. Matsuda, K. Saito, T. Yamamoto, H. Okino, O. Sakata, and S. Kimura, "Dependence of electrical

properties of epitaxial $Pb(Zr,Ti)O_3$ thick films on crystal orientation and Zr/(Zr+Ti) ratio," J. Appl. Phys. **98**(9), 1–8 (2005).

[24] A. Roy Chaudhuri, M. Arredondo, A. Hähnel, A. Morelli, M. Becker, M. Alexe, and I. Vrejoiu, "Epitaxial strain stabilization of a ferroelectric phase in $PbZrO_3$ thin films," Phys. Rev. B **84**(5), 1–8 (2011).

[25] S. Matzen, O. Nesterov, G. Rispens, J.A. Heuver, M. Biegalski, H.M. Christen, and B. Noheda, "Super switching and control of in-plane ferroelectric nanodomains in strained thin films," Nat. Commun **5**, 1–8 (2014).

[26] J. Ma, Y. Zhu, Y. Tang, M. Han, Y. Wang, N. Zhang, M. Zou, Y. Feng, W. Geng, and X. Ma, "Modulation of charged a1/a2 domains and piezoresponses of tensile strained $PbTiO_3$ films by the cooling rate," RSC Adv. **9**(25), 13981–13990 (2019).

[27] A. Singh, S. Monga, N. Sharma, K. Sreenivas, and R.S. Katiyar, "Ferroelectric, Piezoelectric Mechanism and Applications," J. Asian Ceram. Soc. **10**(2), 275–291 (2022).